Colloquium: Linear in temperature resistivity and associated mysteries including high temperature superconductivity

Chandra M. Varma

Physics Department, University of California, Berkeley, California. 94704, USA

(published 7 July 2020)

Immediately after the discovery of high temperature superconductivity in the cuprates in 1987, properties in the metallic state above T_c were discovered that violated the reigning paradigm in condensed matter physics: the quasiparticle concept due to Landau. The most discussed of such properties is the linear in temperature resistivity down to asymptotically low temperatures, sometimes called Planckian resistivity, above the region of the highest T_c. Similar anomalies have since also been discovered in the heavy-fermion compounds and in the Fe-based superconducting metals, and most recently in twisted bilayer graphene. Innumerable papers in the past three decades have pointed out that the linear in T resistivity and associated properties are a mystery and the most important unsolved problem in condensed matter physics; superconductivity itself is a corollary to the normal state properties. Even in this prolifically investigated field, quantitative experimental results on crucial normal state and superconducting state properties have only recently become available. It is now possible to compare some of the detailed predictions of a theory for the normal and superconductive state in cuprates and in heavy fermions with the experiments. The theory gives the frequency and temperature dependence of various normal state properties and also their measured magnitudes in terms of the same values of two parameters. It also resolves the paradox of d-wave symmetry of superconductivity in the cuprates given that the scattering rate of fermions in the normal state is nearly momentum independent. The same parameters that govern the normal state anomalies are also deduced from the quantitative analysis of data in the superconducting state in cuprates. The simplicity of the results depends on the discovery of a new class of quantum-critical fluctuation in which orthogonal topological excitations in space and time determine the spectra, such that the correlations of the critical spectra are a product of a function of space and a function of time with the spatial correlation length proportional to the logarithm of the temporal correlation length. The fermions scattering with such fluctuations form a marginal Fermi liquid.

DOI: 10.1103/RevModPhys.92.031001

CONTENTS

I. INTRODUCTION

Figure 1 presents a schematic universal diagram for the thermodynamically significant phases in the hole-doped cuprates and for the Fe-based superconductors. The phase diagram for several heavy-fermion compounds (von Löhneysen *et al.*, 2007) is similar to the Fe-based superconductors with the structural transition missing. In the cuprates, the Mott-insulating antiferromagnetic phase near half filling of the only band that crosses the Fermi- surface in one-electron calculations (Mattheiss, 1987) gives way with doping to the superconducting phase of d-wave symmetry at low temperatures. Besides the superconducting phase, we focus on the region that begets it: the region marked as I, which is often called the *strange metal*. This region is bounded on one side by a wide crossover to a region that has properties of a Landau Fermi liquid, and no profound problems are raised by it. On the other side is a region marked by an unusual phase transition ending at a quantum-critical point in the superconducting dome. It was realized early on that fundamental new principles must be involved in understanding the strange metal region whose properties are due to the breakdown of the quasiparticle concept, and tentative directions of future research were laid out (Anderson, 1987; Varma *et al.*, 1989). Some prominent reviews along different

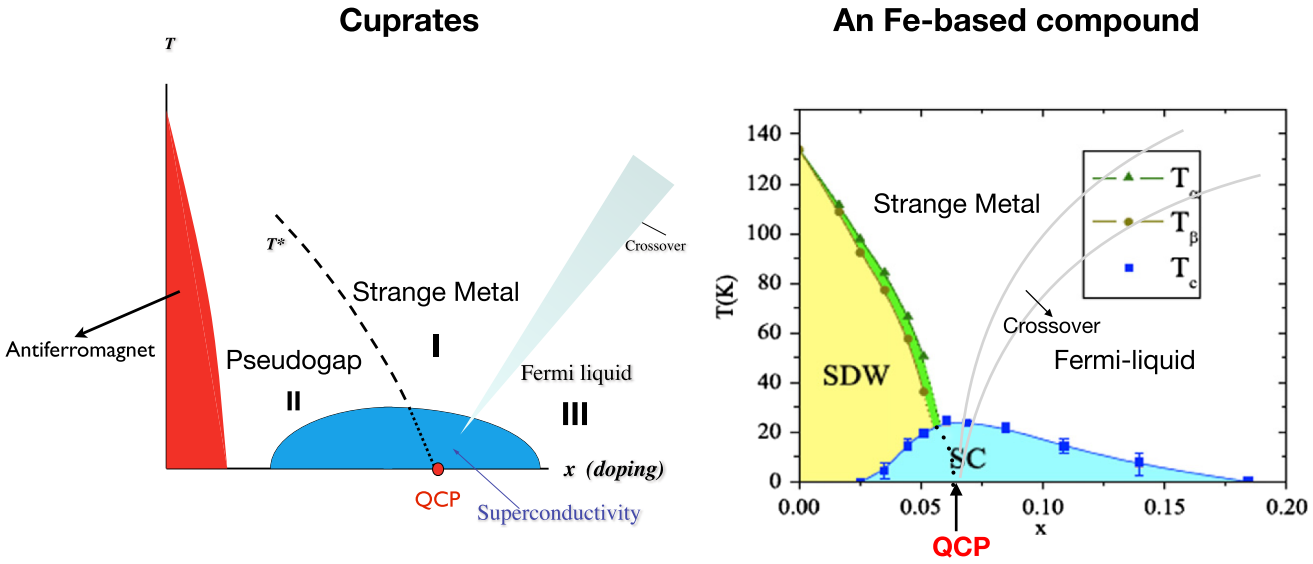

FIG. 1. Schematic universal phase diagrams (left panel) of hole-doped cuprates and (right panel) of the Fe-based compound, based on the data on $Ba(Fe_{1-x}Co_x)_2As_2$ from Chu *et al.* (2009). The quantum-critical point discussed in the text for both is indicated. The wide crossover to Fermi liquid is indicated only roughly for each. In the cuprates, depending on the compound a variety of other thermodynamically small transitions are seen in the pseudogap state below the phase boundary marked T^* as well as a spin-glass state at low temperatures from the antiferromagnetic region to near the quantum-critical point. These are not shown. It has not been clear from experiments where the line marked T^x ends at low doping. In theory, it persists to zero doping.

lines than this Colloquium were given by Anderson (1997), Lee, Nagaosa, and Wen (2006), and Scalapino (2012). Not surprisingly, given the significant attention devoted to this problem by physicists from a variety of different backgrounds, other novel points of view have also been developed. These include a branch of string theory, physics of black holes, and applications of the theory of quantum chaos; see, for example, Zaanen *et al.* (2015), in which these points of view are summarized.

The aim of this Colloquium is to compare detailed quantitative predictions of a theory with a variety of different experiments. The theory is quite subtle and relies on quantum criticality governed by topological excitations. The answers are unusual but, typical of most subtle problems, extraordinarily simple. The model solved is the dissipative 2D quantum XY model and the coupling to fermions of its fluctuations. The model has been solved using renormalization group methods (Hou and Varma, 2016) as accurately as the Kosterlitz solution of the classical XY model (Kosterlitz, 1974), and checked in detail by quantum Monte Carlo calculations with some additional results (Zhu, Chen, and Varma, 2015; Zhu, Hou, and Varma, 2016). The applicability of the model to the quantum criticality of the cuprates and to anisotropic antiferromagnets has also been discussed (Varma, 2015; Varma, Zhu, and Schröder, 2015). A review of the theory was given by Varma (2016). Details of the theory are not given here; only the motivation for the direction of pursuit of the theory and its principal results are summarized. The emphasis in this Colloquium is on a quantitative comparison of the predictions with four different experiments in region I of cuprates in Fig. 1, which was not possible earlier because, even for this prolifically examined problem, some crucial experimental results have become available only in recent years. The most important question in superconductivity, its symmetry and the deduced parameters determining the high T_c, are also given by the theory.

The four different experimental results emphasized are (i) the recent measurement of the $T \ln T$ specific heat on a vertical line above the quantum-critical point marked in Fig. 1, (ii) the measurement of the single-particle scattering rates, (iii) the recently measured density fluctuation spectrum, and (iv) the long-standing results on the linear temperature dependence of the resistivity. It is shown that a new class of theory in quantum criticality gives the temperature and frequency dependence of each of them, and the magnitudes of all four with one dimensionless coupling parameter. These low frequency or temperature dependences persist to an upper cutoff that is measured to be about the same as the singularity in the specific heat or the saturation of the single-particle self-energy. The same two parameters are deduced in the analysis of results of photoemission experiments to give d-wave superconductivity and its transition temperature. The coupling parameter and the cutoff has been estimated in the microscopic theory to within a factor of 2 (Aji, Shekhter, and Varma, 2010).

Some essential aspects of the fluctuation spectra based on a close reading of a variety of experiments were suggested much earlier (Varma *et al.*, 1989), before the microscopic basis was understood and an appropriate theoretical framework for deriving the results was formulated. Now that the foundations of the unusual criticality have been found, many important aspects have changed. But one of the central results, that the fermions form a *marginal Fermi liquid*, which followed from the assumed quantum-critical spectra, remains unchanged.

Related to the physics of the normal state anomalies is the aspect of the theory giving a quantitative theory of the d-wave superconductivity in these compounds (Aji, Shekhter, and Varma, 2010). As we discuss later, given the angle dependence of the single-particle scattering rate, which is quite unlike the hot-spot dominated scattering of conventional

antiferromagnetic fluctuations, *d*-wave superconductivity can occur only if the coupling of the critical fluctuations to fermions has a unique signature given by the theory. Moreover, the same two parameters with which various normal state properties are fitted are deduced from an analysis of angle-resolved photoemission data in a cuprate (Bok *et al.*, 2016).

It is obvious, upon looking at the phase diagrams for Fe-based compounds and heavy fermions in Fig. 1, that the breakdown of the quasiparticle concepts and the superconductivity in them are related to the quantum-critical fluctuations of antiferromagnetism. For the cuprates, the problem is more subtle. Not only is the antiferromagnetic phase often well separated from the region of criticality, the antiferromagnetic correlation length in the region of the highest T_c is measured in some compounds (Balatsky and Bourges, 1999) to be no more than a lattice constant. For the cuprates, the theory of criticality rests on an elusive proposed order breaking time reversal and inversion in the underdoped phase that abuts the quantum-critical region in the phase diagram. The phase transition to such a broken symmetry has been observed in a variety of experiments that are summarized in Sec. III. The model for quantum-critical fluctuations of such an order, discussed in Sec. III.B, is the dissipative quantum XY model. This model can essentially be solved exactly, and the results for scattering from the fluctuations of this model form the backbone of much of the comparison of the experimental results with the theory reviewed in this Colloquium. For the Fe compounds and the heavy fermions, the well developed theory of quantum-critical fluctuations for antiferromagnetic order (Hertz, 1976; Moriya, 1985), which are extensions of classical critical fluctuations to dynamics (Hohenberg and Halperin, 1977), fail to give the observed quantum-critical properties that are essentially identical to those of the cuprates. It has been argued that because of anisotropy, the statistical mechanical model for criticality in these compounds also maps to the quantum XY model. This raises an important unresolved issue that we later describe.

For the cuprates, some important properties, such as the "Fermi arcs" and magneto-oscillations with a small Fermi surface in region II of the phase diagram remain unexplained by the proposed phase. An extension of the broken symmetry to a large period phase was suggested recently (Varma, 2019) to explain these, but it has not yet been tested in proposed experiments. Only when this extension is verified and such properties explained can one claim to have a complete theory of the cuprates.

This Colloquium is organized as follows. In Sec. II, the four classes of normal state experiments mentioned and the deduction of the crucial two parameters determining their magnitude and of *d*-wave superconductivity are summarized. In Sec. III, the results of the theory are summarized to show how the frequency and temperature dependence in each of the experiments is obtained and why two parameters describe all of them quantitatively. In Sec. IV, important unresolved problems are mentioned.

II. EXPERIMENTAL RESULTS

A. Specific heat near quantum criticality

An antiferromagnetic quantum-critical point for the heavy fermions and the Fe-based compounds is evident, and there is no question that the anomalous properties that occur are associated with it. In the hole-doped cuprates, the antiferromagnetic correlation length in the region of the linear in T resistivity and other anomalous properties is only of the order of a lattice constant (Balatsky and Bourges, 1999). A phase diagram with a quantum-critical point in this region (associated with a much different phase transition) was proposed for the cuprates (Varma, 1997), with a line of transitions at the onset of the so-called pseudogap phase. Such a line is now widely accepted. However, the clearest thermodynamic evidence for quantum criticality was discovered only recently through the measurement of the specific singularity in the measured specific heat (Michon *et al.*, 2019) of the algebraic form predicted in 1989 (Varma *et al.*, 1989). Figure 2) from Michon *et al.* (2019), presents the singularity in the specific heat close to the critical point in a measurement down to 0.5 K together with the crossover in the singularity on either side of the quantum-critical point. This measurement was possible because in the compounds measured $La_{2-p}A_pCuO_4$, with $A =$ Nd or Eu, T_c is low enough to be completely suppressed with fields of about 15 T.

Close to quantum criticality, the electronic specific heat fits

$$\frac{C_{\rm el}}{k_B T}(p_c) = \gamma\left[1 + \bar{g}\ln\left(\frac{\bar{T}_x}{T}\right)\right]. \tag{1}$$

The logarithmic enhancement of the specific heat is equivalent to the basic postulates of a marginal Fermi liquid (Varma *et al.*, 1989), that the quasiparticle residue goes to zero at the critical point as

$$z_{\hat{p}}(\omega, T) = \frac{1}{1 + g_{\hat{p}}\ln(\pi T_{x\hat{p}}/x)}, \qquad x = \max(\pi T, \omega). \tag{2}$$

Following the summary of the theory in Sec. III, I assume that both the coupling constant g and the cutoff T_x may have weak dependence on the direction of the momentum $\mathbf{p}$ at the Fermi surface. The experimental $\bar{g}$ and $\bar{T}_x$ in the specific heat may be taken as the averages of the parameters in $z_{\hat{p}}$.

What is plotted in Fig. 2 is not the total specific heat divided by T but $C_{\rm el}/T$ obtained by subtracting from the total specific heat at a given p all but an observed constant electronic or Fermi-liquid contribution to the total specific heat C_v/T at $p = 0.16$. Both are measured at a magnetic field of 8 T to eliminate superconductivity. This serves to eliminate the nuclear Schottky contribution and the phonon contribution. Using $\gamma \approx 5$ mJ/mole K^2 at $p = 0.24$, we may read $\bar{g}$ and the cutoff $\bar{T}_x$ from the slope and the intercept by extending the dashed line to 0 in the right panel of Fig. 2 to be

$$\bar{g} \approx 0.4 \pm 0.1, \qquad \bar{T}_x \approx 1200 \pm 300 \text{ K}. \tag{3}$$

The error bars come from the large region over which an extrapolation is necessary to deduce T_x and the smaller uncertainty in γ.

From Fig. 2, one can also deduce the crossover temperature $\xi_T^{-1}(p - p_c)$ to a Fermi liquid

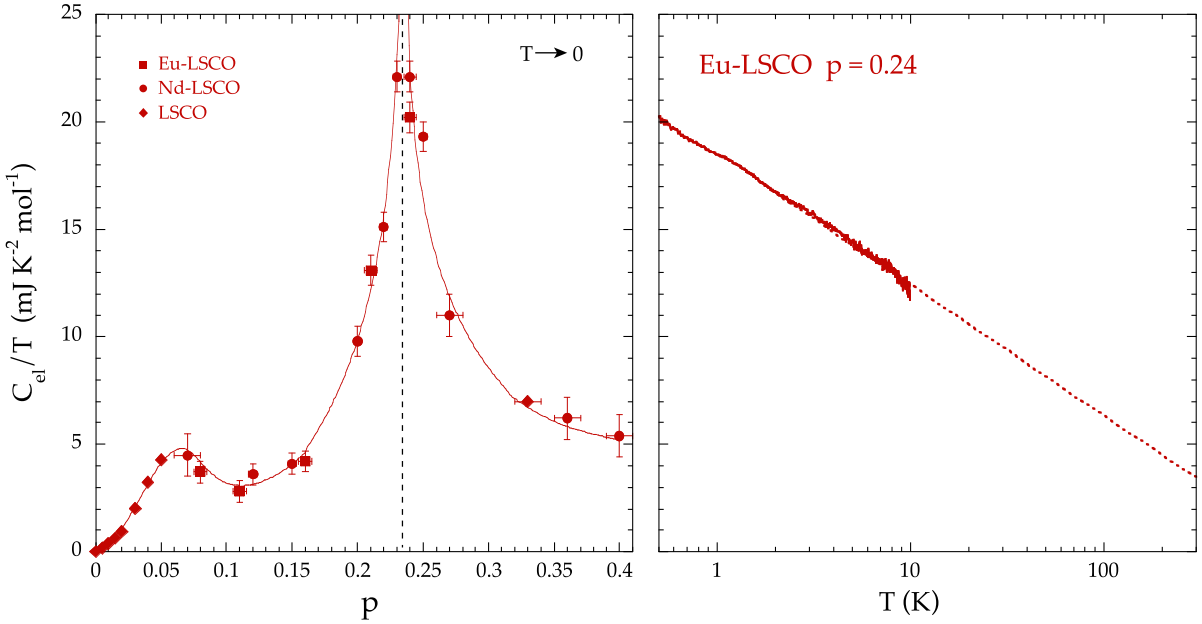

FIG. 2. The electronic specific heat in $La_{2-p}A_pCuO_4$. (Left panel) Data at 0.5 K, the lowest temperature measured (in a magnetic field to remove superconductivity). (Right panel) Temperature dependence of the specific heat nearest the critical composition $p \approx p_c$. From Michon *et al.*, 2019.

$$\frac{C_{\rm el}}{T}(p) = \gamma\left\{1 + \bar{g}\ln\left[T_x \Big/ \sqrt{T^2 + \xi_T^{-2}(p)}\right]\right\}, \tag{4}$$

$$\frac{(\xi_T)^{-1}}{T_x} \propto \left(\frac{p - p_c}{p_c}\right)^{\zeta}. \tag{5}$$

Given the error bars, ζ cannot be determined accurately. Assuming that the background specific heat coefficient γ is independent of T for p ranging between 0.24 and 0.35, $\zeta \approx 0.5$ is estimated. The calculations summarized in Sec. III do give this value.

The $T \ln T$ contribution to the specific heat in one heavy-fermion compound in the region of its linear in T resistivity is quantitatively discussed later. It is helpful if specific heat is measured in the quantum-critical region in other cuprates with low T_c such as Bi2201. In the compounds measured as well as in others, there is a need to measure several dopings close to the critical point to evaluate the crossover regime quantitatively. The effect of the magnetic field on the criticality also needs to be studied carefully.

B. Single-particle relaxation rate

Inelastic single-particle relaxation rates began to be reliably measured in 2000 (Valla *et al.*, 2000) and showed a relaxation rate proportional to T for T much larger than ω and proportional to ω in the opposite limit and with evidence that it is nearly independent of momentum both perpendicular to the Fermi surface and along the Fermi surface. The most complete such measurements arrived in 2005 (Kaminski *et al.*, 2005). I show the relaxation rate in different directions on the Fermi surface for $\omega \gg T$ in Fig. 3. Later measurements showed a relaxation rate about 20% smaller (Bok *et al.*, 2010). Similar results have been obtained by other investigators; for a review, see Damascelli, Hussain, and Shen (2003). The deduction of the single-particle relaxation rate as a function of frequency, in other words, the imaginary part of the single-particle self-energy $\mathrm{Im}\Sigma(\mathbf{p}, \omega)$ reproduced in Fig. 3, is from the energy dependence of the momentum distribution curves, which are also shown in the figure for various energies. Fits to the energy distribution curves for fixed momenta, also given by Kaminski *et al.* (2005), provide results consistent with the parameters deduced. The momentum distribution function fits a Lorentzian well. The Lorentzian form is evidence that the relaxation rate is independent of momentum perpendicular to the Fermi surface (Abrahams and Varma, 2000). To convert to the scattering rate as a function of energy, one must multiply by the band-structure velocity at the measured ω. The low frequency departure from linearity as a function of ω is due to impurity scattering and finite temperature. The data also allow one to deduce a frequency- and temperature-independent relaxation rate that is angle dependent. It is not possible in this experiment to disentangle the small angle impurity scattering contribution (Abrahams and Varma, 2000) and the angle-dependent width due to bilayer splitting in this quantity.

The parameter $b = 0.7 \pm 0.1$ shown in Fig. 3 is independent within this error bar of the momentum along the Fermi surface. It is defined through $\mathrm{Im}\Sigma = a + b\omega$ in the legend in the figure. Given the definition of the parameter $g_{\hat{p}}$ in Eq. (2), $b = (\pi/2)g_{\hat{p}}$. This experiment therefore determines that $\bar{g} = 0.4 \pm 0.1$. This should be compared with $\bar{g}$ deduced from the specific heat in Eq. (3). We must remember that the specific heat is measured in a different compound than the scattering rates. However, when a variety of compounds are measured, as in the resistivity results (Legros *et al.*, 2019) quoted later, the variation of this parameter appears to be no more than 50%. The measurements of the single-particle line shapes in $La_{2-x}Sr_xCuO_4$ (Chang *et al.*, 2007; Zhu *et al.*, 2008) show angle dependence in the scattering rate increasing by about 50% from the (π, π) to the $(\pi, 0)$ directions with a value in the former about the same as that shown in Fig. 3.

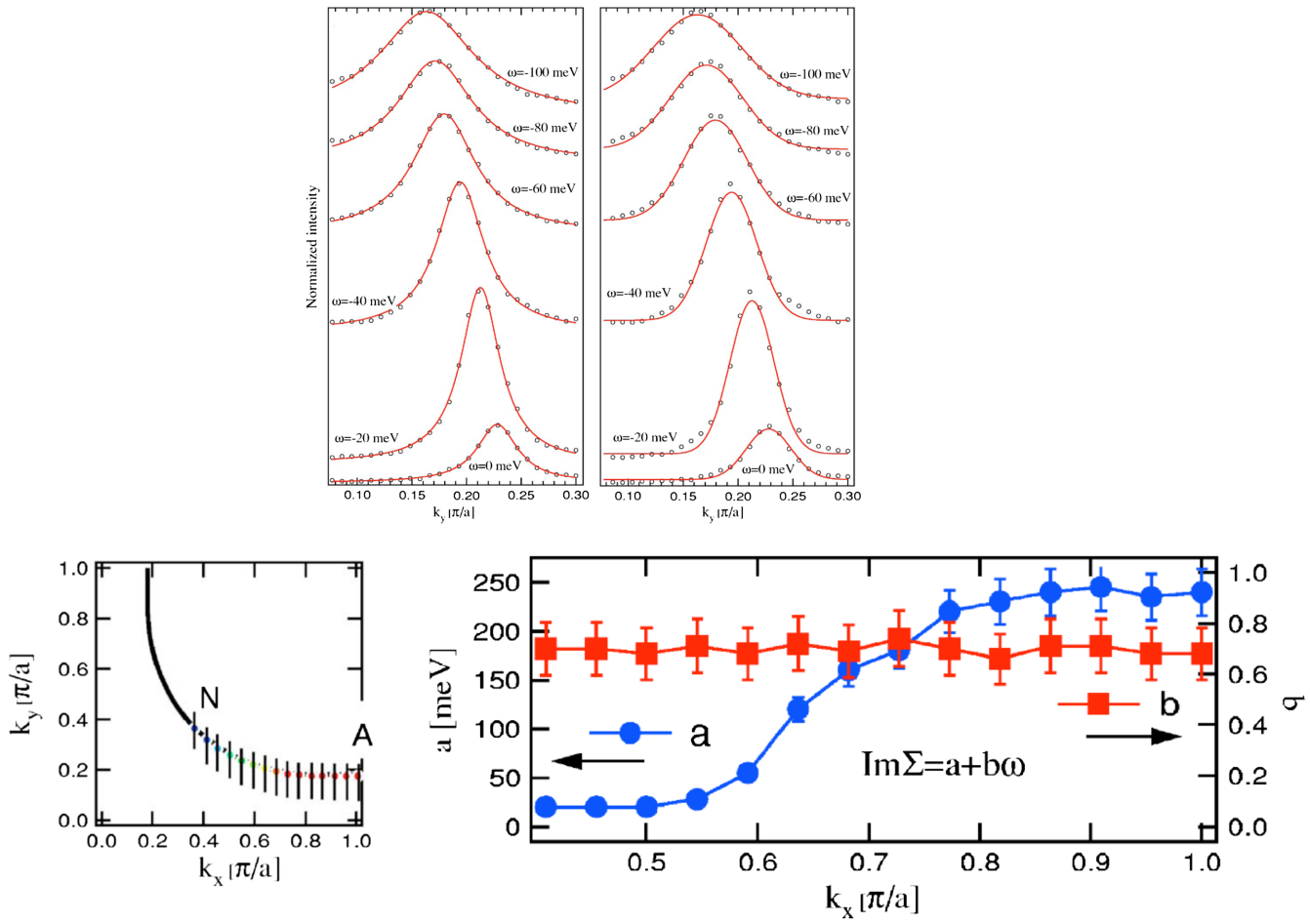

FIG. 3. Single-particle scattering rate measured by ARPES. (Top panels) Momentum distribution curves at various energies with a fit from which the parameters of the self-energy are extracted. The data are fit by red curves that are Lorentzians, proving that the scattering rate is independent of momentum perpendicular to the Fermi surface. (Bottom left panel) The points on the Fermi surface and the directions in which the data were taken. (Bottom right panel) The extracted parameters for the self-energy. From Kaminski *et al.*, 2005

Figure 4 shows a compilation of data of the linewidth in the momentum distribution for a fixed frequency up to frequencies of about 0.5 eV in three different compounds that are measurable by ARPES. The low frequency departure from linearity as a function of ω is due to impurity scattering and finite temperature. The upper cutoff in the relaxation rate given by the theory, when it must change to being frequency independent, is within 50% of the πT_x in the specific heat data shown in Fig. 2. Later measurements in Bi2212 showed (Bok *et al.*, 2010) that this upper cutoff is angle dependent: about 0.5 eV near the diagonal and decreasing to about 0.2 eV in the $(\pi, 0)$ directions. Below about 0.4 eV, the cutoff is the same as the bottom of the band measured from the chemical potential (Kaminski *et al.*, 2005).

C. Resistivity

Figure 5 presents the region of temperature as a function of doping p in $La_{2-p}Sr_pCuO_4$, in which the resistivity is linear in T (Hussey *et al.*, 2011). The dashed lines give the temperature below which resistivity begins to deviate from linear in T. The dashed line on the right marks the temperature cutoff $\xi_T^{-1}(p - p_c)$.

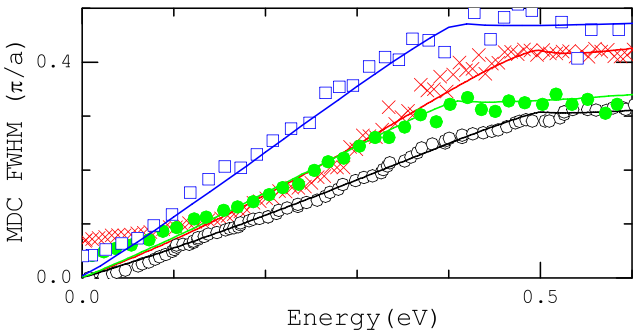

FIG. 4. The full width of the Lorentzian momentum distribution curves as a function of energy up to high energy for the three compounds that were measured by ARPES. The open black circles are data for optimally doped Bi2201 [nodal cut, from Meevasana *et al.* (2008)]. The red crosses are for "optimally doped" Bi2212 [nodal cut, from Graf *et al.* (2007)]. The solid green circles are for $La_{2-p}Sr_pCuO_4$ for $p = 0.17$ at about 20° from the nodal direction, and the blue squares are for the same compound at $p = 0.145$ from the nodal direction. The last two set of points are from Chang *et al.* (2007).

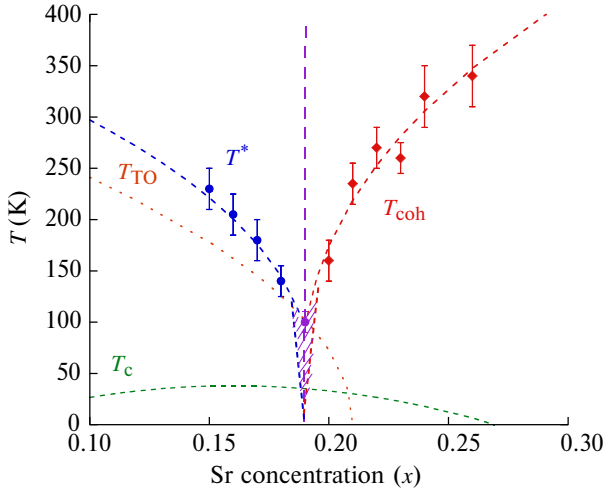

FIG. 5. The resistivity "phase diagram" for $La_{2-x}Sr_xCuO_4$. The temperature dependence of the resistivity begins to show departure from linearity below the lines marked $T^*(x)$ and $T_{\rm coh}$. In this Colloquium, we are concerned with the latter. This line may be fitted with $(x - x_c)^{0.5}$, just as the crossover line in the previously mentioned specific heat data. From Hussey *et al.*, 2011.

The data are consistent with linear in T resistivity to arbitrary low temperatures near the critical doping and in many compounds remain the same up to temperatures at which they begin to melt or decompose, about 1000 K. Recently data from several compounds have been collected (Legros *et al.*, 2019) and summarized after a careful estimate of parameters such as electron density and velocity in terms of a transport relaxation rate

$$\tau_{\rm tr}^{-1} = \alpha k_B T/h \quad \text{for } p \approx p_c. \tag{6}$$

I identify

$$\alpha \equiv (\pi/2) g_{\rm tr}, \tag{7}$$

where $g_{\rm tr} \propto g$; their relation is discussed in Sec. III. There is one fault in the deduction of the dimensionless parameter α given by Legros *et al.* (2019). The effective mass in the formula for conductivity should be the band-structure mass and not the renormalized many body mass, which occurs, for example, in the specific heat. This follows from the Ward identity (Noziéres, 1960; Prange and Kadanoff, 1964; Varma, 1985; Miyake, Matsuura, and Varma, 1989) that is a consequence of the continuity equation. This is a subtle point that is dealt with in Sec. III. Here I simply note that if a renormalized mass were to be used that is logarithmically divergent at criticality at low temperatures, the resistivity would not be linear in temperature but proportional to $T \ln T$ in the quantum-critical region, which can be excluded. Moreover, even if only a constant mass enhancement factor is put in as done by Legros *et al.* (2019), the momentum transport scattering rate would be significantly larger than the single-particle scattering rate. The general theorem is that the transport scattering rates must always be smaller than or equal to the single-particle scattering rates, as discussed in Sec. III. As explained later, the Kadowaki-Woods relation (Kadowaki and Woods, 1986) between the resistivity and specific heat of heavy fermions and others $\rho(T) \propto T^2$ would not be followed. Instead it would be $\rho(T) \propto T^3$. The correct estimate of α is about a factor of 3 [the effective many body enhancement estimated by Legros *et al.* (2019)] lower than that given by Legros *et al.* Legros *et al.* (2019) found α varying in different cuprate compounds to be 0.7 ± 0.2 to 1.2 ± 0.3. The corrected value then varies from about 0.25 ± 0.1 to about 0.4 ± 0.1. $g_{\rm tr}$ is then about $2/3$ of these numbers. $g_{\rm tr}$ is in fact calculated to be about $(2/3)\bar{g}$ in Sec. III, which is quite consistent with the single-particle scattering rates and the specific heat. The resistivity phase diagram in Fig. 5 should be compared with Fig. 2 for specific heat near criticality. More data near the critical point would be helpful. Given what we have, one may deduce a similar value of the crossover exponent $\zeta \approx 0.5$ from this plot as well.

1. Minimum scattering length

As mentioned, the single-particle scattering rate gives an upper limit to the transport scattering rate or the inverse width of the momentum distribution function gives a minimum limit to the transport scattering length $\ell_{\rm tr}$. The maximum in the width of the momentum distribution may be read from Fig. 4. It is about 0.4 (π/a) at an energy of about 0.4 eV (corresponding to a temperature ω_{cx}/π of about 1600 K). The single-particle mean free path ℓ is the half-width and k_F is about $0.8\pi/a$ near critical doping. The concerns that the transport mean free path obtained from resistivity $\ell_{\rm tr}$ is such that $k_F \ell_{\rm tr}$ or $\ell_{\rm tr}/a$ is smaller than 1, the so-called Mott-Ioffe-Regel limit are therefore unfounded. [If the resistivity per 2D conducting layer in the cuprates is written as $(h/2e^2)(1/k_F \ell_{\rm tr})$, the estimated $\ell_{\rm tr}$ (Legros *et al.*, 2019) is nearly the same as ℓ for the same compound.] We appear to be a factor of about 5 on the safe side. The basis of the Ioffe-Regel limit is the uncertainty principle used in deriving it at low temperatures; its use at high temperatures needs study.

D. Density correlations

Significant technical developments have led to a laboratory instrument (Mitrano *et al.*, 2018) to measure the density correlations accurately over a wide range of frequencies and over the entire Brillouin zone. These are shown in Fig. 6. Quite generally, the Einstein relation gives the conductivity

$$\sigma(\omega, T) = e^2 \kappa(T) D(\omega, T). \tag{8}$$

κ is the compressibility, which is equal to the density of states at the Fermi surface for noninteracting fermions for $T \ll E_F$. $D(\omega, T)$ is the diffusion function. A continuity equation gives the imaginary part of the screened density correlation function $\Pi''(q, \omega)$ for $v_F q \ll \omega$:

$$\Pi''(q, \omega) = \frac{\kappa q^2 D(\omega)}{\omega}. \tag{9}$$

The possible quantum-critical aspects arise in the possible renormalization of κ and the frequency dependence of the diffusion function $D(\omega)$. One can write

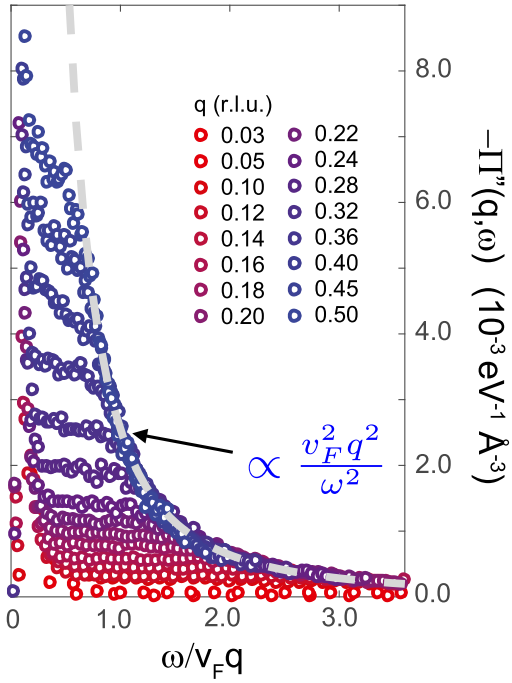

FIG. 6. The imaginary part of the "neutral" density-density correlation function for the region $v_F q/\omega \lesssim 1$ showing the fit to the square of this quantity whose coefficient is related to the compressibility and the scattering rate using the Einstein relation. From Mitrano *et al.*, 2018.

$$D(\omega) = \frac{v_F^2}{2}\tau_{\mathrm{tr}}(\omega), \tag{10}$$

again with no renormalization in v_F from its band-structure value, where τ_{tr} is the transport relaxation rate. Equation (9) is appropriate when the velocity is isotropic. When it is anisotropic, an appropriate average is called for which takes into account the direction of measurement of the density correlations.

Given $\tau_{\mathrm{tr}}(\omega) \propto \omega^{-1}$, $\Pi''(q,\omega) \propto q^2/\omega^2$ follows. This is consistent with the optical conductivity if the conductivity is $\propto 1/\omega$ in the range of the data. (Actually, both the logarithmic dependence of the mass and the upper cutoff begin to play a visible role in the optical conductivity above a frequency of about 0.1 eV, but within the accuracy of the density correlation function data they are unimportant.)

To compare quantitatively, the experimental results shown in Fig. 6 are fitted to find

$$\Pi''(q,\omega) = (3 \pm 0.5) \times 10^{-3}\ \mathrm{eV}^{-1}\,\mathrm{Å}^{-3}\left(\frac{v_F q}{\omega}\right)^2. \tag{11}$$

A bare Fermi velocity of about 2 eV Å obtained from ARPES measurements is used to get this result. The numerical coefficient then is equal to $\kappa(\pi/2)g_{\mathrm{tr}}/2$. The theory of the density correlations in the limit $v_F q/\omega \ll 1$ (Shekhter and Varma, 2009) summarized later allows no singular corrections to the compressibility, but Fermi-liquid corrections are allowed. With the dimensionless g_{tr} from the resistivity measurements of about 0.3, we get $\kappa \approx 10^{-2}/(\mathrm{eV\,Å}^3)$. An unrenormalized κ is the density of states near the chemical potential. Such a density of states is about $2\,\mathrm{states}/[2\,\mathrm{eV}(16\times 12)\ \mathrm{Å}^3] \approx (1/2)\times 10^{-2}/(\mathrm{eV\,Å}^3)$.

Actually, Eq. (9) is obeyed up to nearly $v_F q = \omega$, below which it is nearly a constant (Mitrano *et al.*, 2018). The constant part is indeed even more noteworthy than the part discussed previously. Varma (2017) provided a theory on that.

E. Symmetry of superconductivity in cuprates and parameters determining T_c

Superconductivity of d-wave symmetry is observed in the cuprates. d-wave pairing requires scattering of fermions on the Fermi surface to be predominantly through $\pm\pi/2$ (Miyake, Schmitt-Rink, and Varma, 1986). It is axiomatic that the same fluctuations that dominantly scatter fermions in the normal state are responsible for pairing the fermions. This poses a paradox in cuprates because, as we see in Fig. 3, the single-particle scattering rate is nearly isotropic. The solution to this paradox has been provided (Aji, Shekhter, and Varma, 2010) and is summarized in Sec. III. Its experimental verification comes through analysis of ARPES experiments in the superconducting state (Bok *et al.*, 2016), where the spectral function of the fluctuations in both the superconductivity and the normal state scattering rates were both determined, as well as the symmetry of the coupling functions in the normal and pairing channels and the parameters for the spectral functions and the coupling functions. The experiments were done on a sample of Bi2212 with a T_c of 90 K. It was explained by Bok *et al.* (2016) that the flat frequency dependence of the theoretical and experimentally deduced quantum-critical fluctuation spectra, which is further described in Sec. III, leads to an enhancement for the effective dimensionless parameters $\lambda_{s,d}$ for pairing by a factor of ≈ 3 over g. This comes about because the parameters $\lambda_{s,d}$, the s wave and d wave for interactions in the s-wave and d-wave pairing channels [given by Eq. 1 in Bok *et al.* (2016)] are g multiplied by an integral over all ω of the appropriate angular averages, respectively, of the spectral weight of fluctuations divided by ω. The spectrum is deduced to be essentially ω independent up to the upper cutoff $\omega_c \approx 0.25$ eV. Thus, $\lambda_{s,d} \approx g \ln(\omega_c/T_c)$. Therefore, the deduced $\lambda_{s,d} \approx 1.2$ corresponds to $g \approx 0.4$ for $T_c \approx 90$ K.

The large value of the cutoff and the logarithmic enhancement of the coupling constant for the pairing are crucial for the high T_c in the quantum-critical region.

F. Resistivity and specific heat in heavy fermions and Fe-based compounds

The temperature-dependent resistivity proportional to T has been measured from 30 mK to about 0.6 K in the antiferromagnetic (AFM) quantum-critical region of the compound $CeCu_{6-x}Au_x$ at $x = 0.1$ with crossover on both sides (von Löhneysen *et al.*, 2007). Correspondingly, the specific heat follows Eq. (1) with crossover on either side; see Fig. 7. From the specific heat, one deduces that $g \approx 0.8$ and $T_x \approx 10$ K. Using an effective Fermi energy of about 20 K corresponding to the background specific heat in the nearby Fermi-liquid compositions, a slope in resistivity of about 0.5 is obtained.

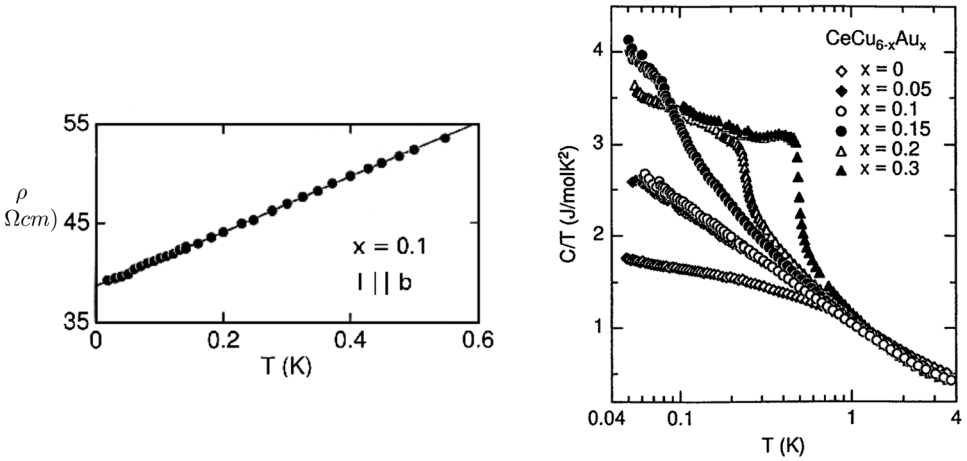

FIG. 7. Resistivity of $CeCu_{5.9}Au_{0.1}$ and specific heat at various pressures and dopings of $CeCu_6$ across the antiferromagnetic quantum-critical point. From von Löhneysen, 1996.

The cutoff T_x is similar to what is directly deduced from the measurements of the fluctuation spectra (Schröder *et al.*, 1998; Varma, Zhu, and Schröder, 2015). The energy scales in this compound are too small to be measured in single-particle spectra by ARPES.

In Fe-based compounds, evidence for the existence of a quantum-critical point (Shibauchi, Carrington, and Matsuda, 2014) has been noted through linear in T dependence of the resistivity. Resistivity for one of the compounds showing one of the clearest linear in T dependences is shown in Fig. 8 together with the thermopower of another that also shows such a resistivity. There is no single-particle spectra to compare with, and neither are the basic band parameters, an average Fermi velocity, etc., known nor a background Fermi-liquid specific heat estimated to get enough parameters to determine g from a scattering rate. Thermopower, which is the entropy per thermally excited particle, does vary as $T \ln T$, which is consistent with the theoretical point of view in this Colloquium. But a quantitative estimate of the parameter g from its magnitude is not possible since there is no estimate of γ. These and the single-particle scattering rates will hopefully be available in the future.

III. FOUNDATION OF THE RESULTS PRESENTED IN A MICROSCOPIC THEORY

The microscopic theory was briefly summarized (Varma, 2016) and detailed references given. Only the motivations for deciding which relevant model to solve, and the principal results from its solution with direct applications to the experiments discussed previously, are discussed now.

A. Order parameter

By the mid 1990s large and universal changes in thermodynamic and transport properties below a line $T^*(p)$ in the phase diagram of the cuprates were observed. The fact that the

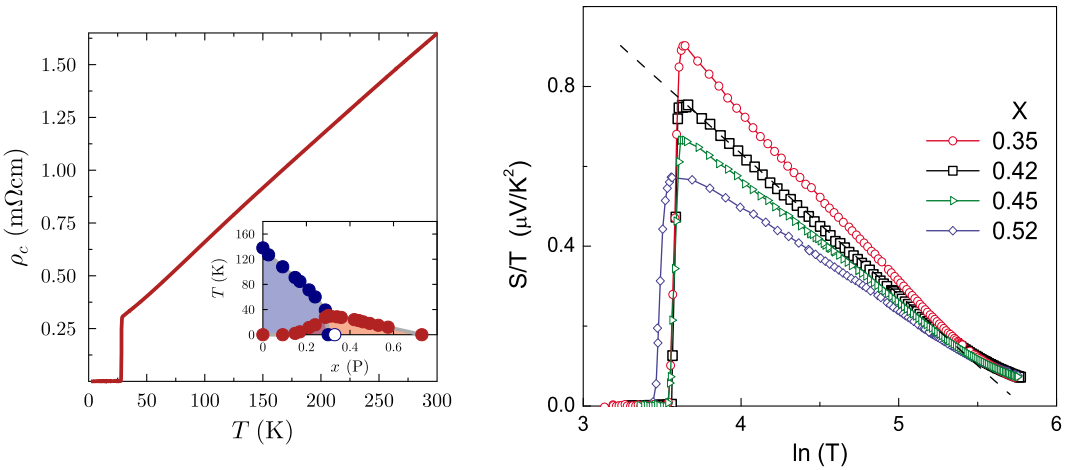

FIG. 8. (Left panel) Phase diagram of $BaFe_2(As_{1-x}P_x)_2$ and resistivity at criticality ($x \approx 0.3$). From Chu *et al.*, 2009. (Right panel) Thermopower S divided by T across AFM quantum criticality in $K_xSr_{1-x}Fe_2As_2$, effectively showing the $T \ln T$ dependence of the specific heat at quantum criticality. Lv *et al.* gave resistivity showing $\propto T$ behavior in a similar range in temperature and composition. From Lv *et al.*, 2009.

region of the quantum fluctuations proposed phenomenologically (Varma *et al.*, 1989) abuts $T^*(p)$ suggests that it was a line of phase transitions to a broken symmetry, which terminates at the quantum-critical point when $p \to p_c$. The order parameter, though it is required to have a condensation energy typically larger than the maximum superconducting condensation energy, has to be unusual so that it was hidden in the experiments carried out. An order parameter was suggested based on mean-field calculations on the three-orbital model for the cuprates (Emery, 1987; Varma, Schmitt-Rink, and Abrahams, 1987) that appeared to satisfy these requirements. The order parameter is depicted on the left in Fig. 9. It preserves translation symmetry and is time reversal and inversion odd but preserves their product. In addition, it is odd in three of the four reflection symmetries of the square lattice. It can be algebraically represented by the magnetoelectric or anapole vector shown in Fig. 9:

$$\mathbf{\Omega} = \int_{\text{cell}} d^2 r [\mathbf{M}(\mathbf{r}) \times \hat{\mathbf{r}}]. \tag{12}$$

The magnetization $\mathbf{M}(\mathbf{r})$ is due to a pair of current loops in each unit cell as shown in the figure. The symmetries broken along the line $T^*(p)$ ending at the quantum-critical point are best observed by polarized neutron scattering (Bourges and Sidis, 2011), although at least five different techniques have led to the observation of at least some of the broken symmetries predicted at the transition (Kaminski *et al.*, 2002; Xia *et al.*, 2008; Leridon *et al.*, 2009; Shekhter *et al.*, 2013; Lubashevsky *et al.*, 2014; Sato *et al.*, 2017; Zhao *et al.*, 2017; Murayama *et al.*, 2018; Zhang *et al.*, 2018; Mukherjee *et al.*, 2019). Neutron scattering experiments (Bourges and Sidis, 2011) have observed changes consistent with the symmetries in Fig. 9 for four different families of cuprates at various p. Figure 9 (right panel) shows the onset temperature of the symmetry changes observed in various experiments in the cuprate most extensively investigated $YBa_2Cu_3O_{6+x}$. The magnitude of the order parameter is typically $0.1\mu_B$ per unit cell. The free-energy reduction due to such an order parameter setting in at 100 K (Varma and Zhu, 2015) is about 3 times that of the maximum superconducting condensation energy near p_c, fulfilling one of the requirements that it be a transition competing with superconductivity and overcoming it at smaller doping.

B. Model and correlation function for quantum fluctuations

The order parameter $\mathbf{\Omega}$ shown in Fig. 9 has four possible orientations in a unit cell. The interactions between cells is among these four possible orientations. The model for the order parameter is therefore the two-dimensional XY model with fourfold anisotropy if one ignores the amplitude fluctuations that are irrelevant in two dimensions. In the classical XY model, the four-fold anisotropy is marginally relevant. But it has been shown to be irrelevant for a quantum phase transition (Aji and Varma, 2007). The classical model has no divergence of the specific heat, consistent with the lack of any sharp signature in the experimental specific heat at $T^*(p)$. The model to be solved then is the quantum XY model in two dimensions, whose fluctuations are coupled to the fermions in the model. An essential aspect of a quantum phase transition in a metal is the dissipation due to decay of the order parameter to

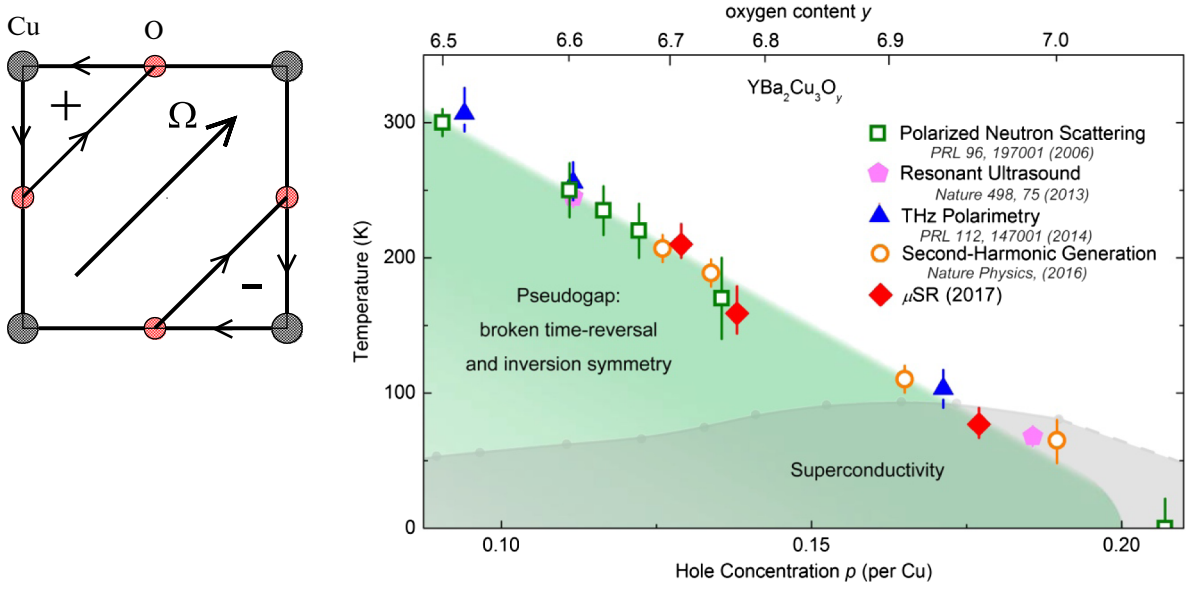

FIG. 9. (Left panel) The order parameter depicted by the vector $\mathbf{\Omega}$ representing the magnetoelectric order parameter of Eq. (12). $\mathbf{\Omega}$ is odd in both time-reversal and inversion and preserves their product. These symmetries come from a pair of spontaneously generated current loops in a Cu-O_2 unit cell. (Right panel) Various experiments showing the onset temperature of symmetries consistent with that mentioned in the compound $YBaCu_3O_{6+x}$. The neutron scattering experiments are from Fauqué *et al.* (2006), the polarimetry experiments from Lubashevsky *et al.* (2014), the second harmonic generation from Zhao *et al.* (2017), the μSR from Zhang *et al.* (2018), and the ultrasound measurements from Shekhter *et al.* (2013).

incoherent degrees of freedom of the same symmetry in the fermions. Thus, the model has the action

$$S = -K_0 \sum_{\langle \mathbf{x},\mathbf{x}' \rangle} \int_0^\beta d\tau \cos(\theta_{\mathbf{x},\tau} - \theta_{\mathbf{x}',\tau}) + \frac{1}{2E_0} \sum_{\mathbf{x}} \int_0^\beta d\tau \left(\frac{d\theta_{\mathbf{x}}}{d\tau}\right)^2 + S_{\rm diss}. \tag{13}$$

$\theta_{\mathbf{x},\tau}$ is the angle of the vector $\mathbf{\Omega}$ in the unit cell at location $\mathbf{x}$ and at imaginary time τ, which is periodic in the interval $(0, \beta = 1/k_B T)$. The first term is the potential energy of the 2D XY model, and the second term is the kinetic energy written in terms of the angular momentum $\mathbf{L}_z = d\theta_{\mathbf{x}}/d\tau$. The third term is the dissipation due to coupling to the fermions. The dissipation is of the Caldeira-Leggett symmetry (Caldeira and Leggett, 1983), which was introduced for the dissipation of current fluctuations proportional to the gradient of the superconducting phase in a bath of current carrying fermions. In this case, its origin is the decay of the collective current proportional to $\nabla\theta(\mathbf{r},\tau)$ or that of the collective angular momentum variable $\mathbf{L}_z(\mathbf{r},\tau)$ into local angular momentum fluctuations of the fermions; for further details, see Varma (2016). Each of the terms of this model has been derived from the three-orbital model (Aji, Shekhter, and Varma, 2010).

The classical XY model was solved analytically by the renormalization group method (Kosterlitz, 1974) after transforming it essentially exactly in to a model for vortices interacting logarithmically in space. The quantum XY model with the action (13) can also be transformed essentially exactly (Aji and Varma, 2007) into a model for vortices interacting logarithmically in space but locally in time even for the quantum model and another set of topological excitations, the *warps*, which interact dominantly through a logarithmic interaction in imaginary time τ but locally in space. This model can also be solved by the renormalization group method (Hou and Varma, 2016). The vortices and warps are orthogonal topological excitations, which is what makes the model soluble. The answers are checked using detailed Monte Carlo calculations (Zhu, Chen, and Varma, 2015; Zhu, Hou, and Varma, 2016) on the original model (13), where evidence for the vortices and the warps and their correlations is directly exhibited.

The correlation function of the operator $e^{i\theta(\mathbf{r},\tau)}$ is calculated in the quantum-fluctuation regime of the model. The most important result is that the correlation functions are products of a function of space and of imaginary time τ and that the spatial correlation length is proportional to the logarithm of the temporal correlation. This leads effectively to relative freedom of the temporal and spatial metric near criticality and to unusual but simple results for physical properties in terms of just two parameters:

$$G(\mathbf{r},\mathbf{r}',\tau,\tau') = \langle e^{i\theta(\mathbf{r},\tau)} e^{-i\theta(\mathbf{r}',\tau')} \rangle \tag{14}$$

$$= G_0 \left(\frac{\tau_c}{\tau - \tau'}\right) [\ln |(\mathbf{r} - \mathbf{r}')/a|] e^{-|\tau-\tau'|/\xi_\tau} e^{-|\mathbf{r}-\mathbf{r}'|/\xi_r}, \tag{15}$$

$$\frac{\xi_r}{a} = \ln \frac{\xi_\tau}{\tau_c}. \tag{16}$$

τ_c^{-1} is the high energy cutoff in the theory ($\omega_{cx} = \pi T_{cx}$ in the analysis of the experiments). The $1/(\tau - \tau')$ dependence can be transformed to Matsubara frequencies that can be analytically transformed to real frequencies to give the function $\tanh(\omega/2T)$. The asymptotic low energy and high energy forms of this were the phenomenological assumption made in 1989 (Varma *et al.*, 1989) for the fluctuation spectra. It is also shown that the spectral fluctuations of the correlation $\langle \mathbf{L}_z(\mathbf{r},\tau)\mathbf{L}_z(\mathbf{r}',\tau')\rangle$ are identical to those in Eq. (14) (Aji and Varma, 2009).

The variation of the correlation length ξ_τ as a function of $p - p_c$ or, equivalently, to the parameters of the XY model has been obtained using quantum Monte Carlo calculations (Zhu, Hou, and Varma, 2016). When the variation is due to the variation in the ratio of the kinetic energy parameter to the interaction energy parameter for a fixed dissipation, the exponent ζ previously defined through the experiments on specific heat and resistivity is approximately $1/2$, which is consistent with the data.

Just like for the classical XY model, quantum-critical fluctuations of the model are unlike the extensions of classical dynamical critical phenomena of models of the Ginzburg-Landau-Wilson class to the quantum regime. This appears to be essential as the conventional critical dynamics of such a class cannot give the observed properties. In such models, the space and time correlations are connected through finite dynamical critical exponents and the scale of both fluctuations diminishes to zero near the critical point. By contrast the temporal fluctuations in Eq. (14) remain on the scale of the cutoff over the entire fluctuation regime and the low energy form has a ω/T scaling. These were essential in the calculations of the observed experimental properties summarized previously as well as for high temperature superconductivity.

C. Coupling function of fermions to the fluctuations

The coupling function of fermions to the quantum-critical fluctuations should be used to calculate both the normal self-energy and the pairing self-energy. It should also be the same function that is used to calculate the dissipation of the quantum-critical fluctuations due to decay into particle-hole pairs. The important coupling of fermions to the fluctuations is deduced as follows. As discussed previously, the critical fluctuations are

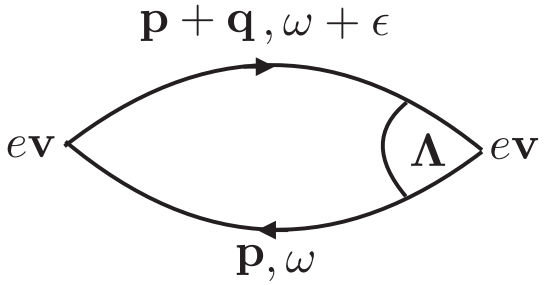

FIG. 10. The Kubo formula for the current-current correlation in terms of the bare current operator, the renormalized current operator and the exact single-particle Green's functions. The dc conductivity is $(1/\epsilon)$ times the imaginary part of the current-current correlation at $\mathbf{q} \to 0$.

also the fluctuations of the collective angular momentum operator $L_z(\mathbf{r},\tau)$. This can couple to fermions only through their local angular momentum operator, with symmetry that of $\ell_z \equiv (1/2)i(\mathbf{r}\times\boldsymbol{\nabla}-\boldsymbol{\nabla}\times\mathbf{r})$. Thus, a Hamiltonian for the scattering of fermion creation and annihilation operators $\psi^+(\mathbf{p},\sigma),\psi(\mathbf{p},\sigma)$ to the fluctuations is derived (Aji, Shekhter, and Varma, 2010) to be

$$H_{\text{coupling}} = \sum_{\mathbf{p},\mathbf{p}',\sigma} \gamma(\mathbf{p},\mathbf{p}')\psi^+_{\mathbf{p},\sigma}\psi_{\mathbf{p}',\sigma}\mathbf{L}_z(\mathbf{p}-\mathbf{p}') + \text{H.c.}, \quad (17)$$

where the coupling function

$$\gamma(\mathbf{p},\mathbf{p}') = i\gamma_0(\mathbf{p}\times\mathbf{p}') \quad (18)$$

is the Fourier transform of the fermion angular momentum ℓ_z. [Aji, Shekhter, and Varma (2010) derived the equivalent of Eq. (17) microscopically for lattice fermions.] The physics of how Eq. (17) leads to d-wave superconductivity and nearly angle-independent normal self-energy is shown in Sec. III.D.3.

D. Calculations of some measurable properties

1. Single-particle self-energy and specific heat

The fluctuations (14) serve as the irreducible vertex (Noziéres, 1960) in a calculation of the properties of fermions. Because of the product form of Eq. (14), the calculations for the properties of fermions can be done easily and precisely (Varma, 2016). Of relevance to this Colloquium is the retarded self-energy of the fermions, which has the full symmetry of the lattice. Since the fluctuations are momentum independent, only the projection of $|\gamma(\mathbf{p},\mathbf{p}')|^2$ to the full symmetry of the lattice appears in the calculation (Aji, Shekhter, and Varma, 2010; Bok *et al.*, 2016), as explained later. For a circular Fermi surface, that is just identity. Then

$$\begin{aligned}\Sigma(\mathbf{p},\omega) &= g_{\hat{\mathbf{p}}}\left[i\frac{\pi}{2}\max(|\omega|,\pi T) + \omega\ln\left(\frac{\omega_{cx}}{x}\right)\right] \\ &\quad \text{for } \max(\omega,\pi T) \lesssim \omega_{cx} \\ &= i\frac{\pi}{2}g_{\hat{\mathbf{p}}}\omega_c \quad \text{for } \max(|\omega|,T) \gg \omega_{cx}. \end{aligned} \quad (19)$$

$g_{\hat{\mathbf{p}}}$ (Aji, Shekhter, and Varma, 2010) is the product of the amplitude of the fluctuations G_0, the density of states of the fermions $N(0)$, and the coupling γ_0^2. It also depends on the anisotropy of the band structure. It is independent of $\mathbf{p}$ for a circular Fermi surface. For the band structure of Bi2212 near optimum doping, it is estimated to increase by less than about 2 in going from the (π,π) directions to the $(\pi,0)$ directions. For a square lattice, the correction to isotropy varies as $\cos 4\theta(\hat{\mathbf{p}})$.

The electronic specific heat can be written directly in terms of integrals over the imaginary part of the self-energy (Abrikosov, Gorkov, and Dzyaloshinski, 1963). The result is particularly simple when the self-energy is nearly momentum independent. Then the specific heat singularity is simply given by the inverse of the renormalization given in Eq. (2), which follows from Eq. (19). There is no renormalization of the compressibility if the self-energy is momentum independent (Varma, 1985).

2. Resistivity

The conductivity may be calculated in three different ways.

(1) From the Boltzmann equation, which simplifies enormously when the self-energy is independent of momentum (Varma *et al.*, 1989). Then the momentum transport scattering rate is equal to the imaginary part of the single-particle self-energy. Thus, the dc resistivity is proportional to T in the quantum-critical region with the same slope as the self-energy for a circular Fermi surface. One may calculate the vertex correction due to the small angular dependence in the self-energy using the Boltzmann equation, for example, as given by Varma and Abrahams (2001) and Abrahams and Varma (2003). The transport scattering rate is then necessarily smaller than the single-particle scattering rate. A straightforward calculation shows that with a factor of 2 variation in the self-energy, increasing in the direction where the velocity is least, the coefficient of the linear in T resistivity is about $2/3$ that of the maximum self-energy.

(2) The density-density correlation has also been calculated directly (Shekhter and Varma, 2009; Varma, 2017), giving the form shown in Fig. 6 with the inverse diffusion coefficient related to the resistivity as noted.

(3) The conductivity may be calculated using the Kubo formula. The Kubo formula for conductivity is equivalent to the evaluation of Fig. 10 for the current-current correlations. The vertex on the left is the bare band-structure velocity operator $\mathbf{v}$, the vertex on the right is the renormalized velocity operator $\mathbf{v}_{\text{renorm}}$, and the lines are the exact Green's functions. In the appropriate limit for the calculation of the dc conductivity, the matrix elements of the operator $\mathbf{v}_{\text{renorm}}$ are given by the Ward identity (Noziéres, 1960) that follows from the equation for continuity:

$$\mathbf{v}_{\text{renorm}} = \boldsymbol{\Lambda}\mathbf{v} \quad (20)$$

$$\lim_{\epsilon\to 0\mathbf{q}\to 0}\boldsymbol{\Lambda}(\mathbf{p},\omega;\mathbf{q},\epsilon) = \mathbf{1} - \frac{1}{\mathbf{v}}\frac{\partial\Sigma(\mathbf{p},\omega,T)}{\partial\mathbf{p}}. \quad (21)$$

If $\Sigma(\mathbf{p},\omega,T)$ is independent of $\mathbf{p}$, the relevant limit $\mathbf{v}_{\text{renorm}} = \mathbf{v}$. The sum over frequencies and integration over momentum over the Green's functions in Fig. 10 can be easily carried out for the same conditions. The conductivity in the α direction is then

$$\sigma_\alpha(T) = \frac{e^2\langle v_\alpha^2\rangle N(0)}{2\text{Im}\Sigma(\mathbf{p}_F,0,T)}. \quad (22)$$

The dc resistivity is proportional to T due to the self-energy in the denominator. To get the coefficient of the resistivity, note that $N(0)$ in Eq. (22) is the bare

(given by one-electron theory band-structure) density of states and $\langle v_\alpha^2 \rangle$ is the bare mean square Fermi velocity in the α direction because of Eq. (20). $N(0)\langle v_\alpha^2 \rangle$ is proportional to the inverse mass. It is for this quantity that often, as shown by Legros *et al.* (2019), a renormalized mass, such as that occurring in specific heat, is used. As shown here, for the conditions of quantum criticality in cuprates, this mass is the bare or band-structure mass. One can show (Varma, 2017) that the lack of any renormalization of the effective mass in the conductivity is true only for frequencies much smaller than the temperature.

This issue also arises in Fermi liquids if the condition that the self-energy is weakly momentum dependent compared to its frequency dependence (Varma, 1985) is satisfied. An application in that case to the resistivity in heavy fermions is given in Eq. (3) of Miyake, Matsuura, and Varma (1989), where the Kadowaki-Woods observation (Kadowaki and Woods, 1986) was derived. For applications to the problems of interest in this Colloquium, the T^2 on the left side of that equation should be replaced by T, and the ImΣ on the right side should be replaced by the relevant part of Eq. (19) to get Eq. (22). If one uses a renormalized value for $N(0)\langle v_\alpha^2 \rangle$, resistivity is not proportional to the square of the specific heat (the Kadawoki-Woods observation) but is proportional to the cube of the specific heat.

For all the properties considered in this Colloquium, there are only two parameters, g and ω_c, in terms of which every property considered is given. These two parameters were estimated by Aji, Shekhter, and Varma (2010) from the kinetic and interaction energies of a copper oxide three-orbital model. This gave $g \approx 1$ and $\omega_c \approx 0.5$ eV, i.e., within about a factor of 2 of the experimentally deduced numbers.

3. Coupling function for *d*-wave superconductivity

Note that with $\mathbf{p}, \mathbf{p}'$ on the nearly circular Fermi surface

$$
\begin{aligned}
&-|\gamma(\mathbf{p},\mathbf{p}')|^2 \\
&\quad = -\gamma_0^2 |i(\mathbf{p}\times\mathbf{p}')|^2 \\
&\quad \propto \frac{\gamma_0^2}{2}[1-\cos(2\theta_p)\cos(2\theta_{p'})-\sin(2\theta_p)\sin(2\theta_{p'})]. \qquad (23)
\end{aligned}
$$

Since in a calculation of the normal state self-energy the intermediate state has the full symmetry of the lattice (see Fig. 11) and the fluctuation spectra is momentum independent, the only angle dependence comes from the projection of the pair of vertices to the full symmetry of the lattice, i.e., of Eq. (23). This yields just $-|\gamma_0|^2$ and is repulsive in the s-wave pairing channel. (The minus sign comes from the loop integral in the diagram for the self-energies.) On the other hand, in the pairing channel of the d-wave symmetry the intermediate state has d-wave symmetry. Thus, a projection of Eq. (23) to the d wave can contribute from the second or third term in it. This is attractive and on a circular Fermi surface would be degenerate between the $d(x^2-y^2)$ state and $d(xy)$. In the cuprates, the density of states is the least in the diagonal direction of the Brillouin zone, favoring thereby the former.

Equation (23) and Fig. 11 explains the principal paradox in superconductivity of the cuprates: while the measured anomalous single-particle self-energy is nearly angle independent, superconductivity of d-wave symmetry occurs.

IV. RELATED MATTERS

It is worth emphasizing the three general features required in the results of a theory for the quantum-critical fluctuations to be relevant to the normal state properties and superconductivity in the materials discussed. (1) The frequency dependence of the absorptive part of the form $\tanh(\omega/2T)$ or, equivalently, the time dependence of the form $1/\tau$ as given in Eq. (14). (2) The fluctuation spectra of a product form of momentum and the previously mentioned frequency dependence as given in Eq. (14). For relevance to superconductivity, it is further necessary (3) that the coupling of fermions be such that the normal state properties are nearly angle dependent but the pairing is in the d-wave channel.

Some prominent reviews of theory with a point of view differing from that presented here were given by Anderson (1997), Lee, Nagaosa, and Wen (2006), and Scalapino (2012). None of them or any other theoretical ideas and calculations on any *physical model* have explained the temperature and frequency dependence of the properties discussed here in cuprates or heavy fermions or the Fe-based compounds, let alone given the parameters or resolved the paradox of the symmetry of superconductivity discussed previously. Calculations that are extensions of the dynamical classical critical phenomena to quantum criticality (Hertz, 1976;

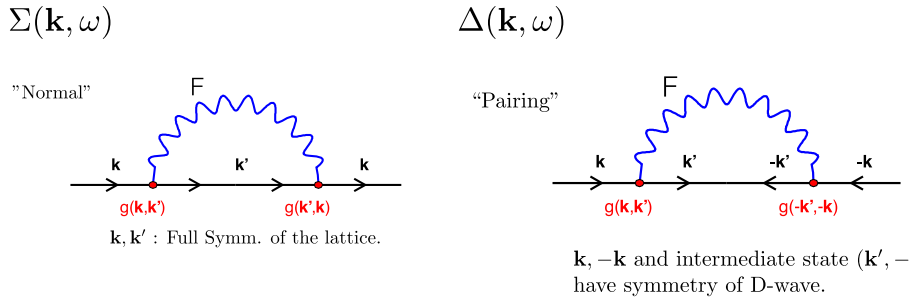

FIG. 11. The skeletal diagrams for the normal self-energy and the pairing self-energy for scattering fermions from fluctuations whose propagator is depicted as a wavy line. The former has the ordinary part of the Gorkov Green's function in the intermediate state and the latter the pairing part. The vertices in the two diagrams are closely related.

Moriya, 1985), and that have been extensively worked on since, are known not to give any of the experimental properties noted. The one that comes the closest is a $(0+1)$-dimensional disordered model of SU(N) spins in the limit $N \to \infty$ (Sachdev and Ye, 1993), which leads to the fluctuation spectra in frequency that was suggested by Varma *et al.* (1989). Besides the difficulty of how such a model could be an effective physical model, it has the problem that an extensive ground state entropy is inevitably tied to its results. Modification of the model to remove this entropy (Chowdhury *et al.*, 2018) also alters its properties to that of a Fermi liquid. Self-consistent single impurity models (Si *et al.*, 2001) have been introduced for heavy-fermion quantum criticality. They do not yield the correct frequency dependence to give the linear in T resistivity.

The prominent shortcomings in the present theory are as follows.

(1) The application of the dissipative quantum XY model to the cuprates is clear given the symmetries changed at $T^*(x)$. The application of the same model is not a surprise close to the AFM critical point in the heavy fermions and the Fe compounds. The anisotropic AFM maps to such a model [see Varma (2015) and the erratum], and the point of view is supported by the fit to the measured fluctuation spectra by the calculated fluctuations (Varma, Zhu, and Schröder, 2015). The unanswered question is why the theory works over such a wide temperature range when the XY anisotropy is so small that the classical transition would crossover to that of the XY model only close to the transition. The answer may lie in the possibility that with criticality of the kind discovered in the model, which for some purposes may be regarded as having a dynamical critical exponent $z \to \infty$, the crossover to the anisotropic model occurs over essentially the entire range below the ultraviolet cutoff. The reason for the speculation is that the crossover temperature in classical critical phenomena is given in terms of the product νz, where ν is the classical correlation length exponent.

(2) A principal problem in cuprates, the understanding of some remarkable properties in the pseudogap state, remains unexplained in the theory described previously (and indeed in any other theory). While a thermodynamically significant phase transition of the predicted symmetry has been discovered at $T^*(p)$, it cannot give the peculiar observed Fermi arcs (Damascelli, Hussain, and Shen, 2003) or the magneto-oscillations of a small Fermi surface (Sebastian and Proust, 2015) because it does not change the translation symmetry of the lattice. Since the only phase transition discovered at $T^*(p)$ is to a phase of the symmetry shown in Fig. 9 and since its fluctuations explain so well both the quantum-critical region and the superconductivity in the cuprates, a modification of the observed order in which a long period wave of the four distinct symmetries shown in Fig. 9 has been suggested (Varma, 2019). This retains the calculated and observed properties discussed in this Colloquium and also is calculated to lead to the unexplained properties (Varma, 2019). The modified phase can, in principle, be discovered by high resolution resonant x-ray scattering. Only after such an observation can one claim that the cuprate problem is solved.

Recently experiments in twisted bilayer graphene revealed a linear in T resistivity (Cao *et al.*, 2019; Lu *et al.*, 2019; Polshyn *et al.*, 2019) in the phase diagram in a region that has the quantum-critical shape in the phase diagram at the boundary between the insulator and the superconductor, extending to asymptotic low temperatures when a magnetic field is applied to suppress superconductivity. One may speculate that the relevant model for critical fluctuations is again of the XY variety, with the U(1) symmetry being that of valley space, which may be broken in the correlated insulator.

I speculate that quantum-critical fluctuations of a variety of soft vertex models coupled to fermions [many of which for 2D classical problems were treated by Baxter (1982)], which classically are not in the Ginzburg-Landau or Wilson-Fisher class, are generically related to the 2D dissipative XY model in the quantum version of the problems. They may all be governed by topological excitations with relative freedom of temporal and spatial fluctuations. The scaling of the metric of space and time that differs from the flat world is the fundamental aspect of any quantum-critical problem. That the spatial and temporal metrics become free relative to each other is a unique property that has led to the simple results that explain the observed quantum criticality in the problems discussed. The model itself is richer than the application noted here. For example, there is a critical region to a phase in it (Zhu, Chen, and Varma, 2015; Hou and Varma, 2016; Zhu, Hou, and Varma, 2016) in which the correlation functions are of product form in space and time but with a temporal correlation length proportional logarithmically to the spatial correlation length. One may speculate, of course at great peril, that this is the appropriate description of another quantum-critical problem: inflation in the early Universe.

ACKNOWLEDGMENTS

I wish to thank the many experimentalists who have taken the time to explain their experimental results to me. The data quoted here are of course a small fraction of the mutually consistent data that exist in the literature. I especially thank Bastien Michon and Louis Taillefer for providing me with versions of figures from their paper suitable for me and for answering questions about the data. This Colloquium was partially written while at the Aspen Center for Physics and finished at the University of California, Berkeley, where I have been a visitor part of the year for the past four years. I thank James Analytis, Robert Birgeneau, Dung-Hai Lee, and Joel Moore at Berkeley for their hospitality.

REFERENCES

Abrahams, E., and C. M. Varma, 2000, "What angle-resolved photoemission experiments tell about the microscopic theory for high-temperature superconductors," Proc. Natl. Acad. Sci. U.S.A. **97**, 5714.

Abrahams, Elihu, and C. M. Varma, 2003, "Hall effect in the marginal Fermi liquid regime of high-T_c superconductors," Phys. Rev. B **68**, 094502.

Abrikosov, A. A., L. P. Gorkov, and I. E. Dzyaloshinski, 1963, *Methods of Quantum Field Theory in Statistical Physics* (Prentice-HallEnglewood Cliffs, NJ).

Aji, Vivek, Arkady Shekhter, and C. M. Varma, 2010, "Theory of the coupling of quantum-critical fluctuations to fermions and *d*-wave superconductivity in cuprates," Phys. Rev. B **81**, 064515.

Aji, Vivek, and C. M. Varma, 2007, "Theory of the Quantum Critical Fluctuations in Cuprate Superconductors," Phys. Rev. Lett. **99**, 067003.

Aji, Vivek, and C. M. Varma, 2009, "Quantum criticality in dissipative quantum two-dimensional *XY* and Ashkin-Teller models: Application to the cuprates," Phys. Rev. B **79**, 184501.

Anderson, P. W., 1987, "The resonating valence bond state in La_2CuO_4 and superconductivity," Science **235**, 1196–1198.

Anderson, P. W., 1997, *The Theory of Superconductivity in the High-T_c Cuprates*, Princeton Series in Physics (Princeton University Press, Princeton, NJ).

Balatsky, A. V., and P. Bourges, 1999, "Linear Dependence of Peak Width in $\chi(q,\omega)$ vs T_c for $YBa_2Cu_3O_{6+x}$ Superconductors," Phys. Rev. Lett. **82**, 5337–5340.

Baxter, R. J., 1982, *Exactly Solved Models in Statistical Mechanics* (Academic, London).

Bok, Jin Mo, Jong Ju Bae, Han-Yong Choi, Chandra M. Varma, Wentao Zhang, Junfeng He, Yuxiao Zhang, Li Yu, and X. J. Zhou, 2016, "Quantitative determination of pairing interactions for high-temperature superconductivity in cuprates," Sci. Adv. **2**, e1501329.

Bok, Jin Mo, Jae Hyun Yun, Han-Yong Choi, Wentao Zhang, X. J. Zhou, and Chandra M. Varma, 2010, "Momentum dependence of the single-particle self-energy and fluctuation spectrum of slightly underdoped $Bi_2Sr_2CaCu_2O_{8+\delta}$ from high-resolution laser angle-resolved photoemission," Phys. Rev. B **81**, 174516.

Bourges, Philippe, and Yvan Sidis, 2011, "Novel magnetic order in the pseudogap state of high-copper oxides superconductors," C.R. Phys. **12**, 461–479.

Caldeira, A. O., and A. J. Leggett, 1983, "Influence of dissipation on quantum tunneling in macroscopic systems," Ann. Phys. (N.Y.) **149**, 374.

Cao, Yuan, Debanjan Chowdhury, Daniel Rodan-Legrain, Oriol Rubies-Bigorda, Kenji Watanabe, Takashi Taniguchi, T. Senthil, and Pablo. Jarillo-Herrero, 2019, "Strange metal in magic-angle graphene with near Planckian dissipation," arXiv:1901.03710.

Chang, J., *et al.*, 2007, "When low- and high-energy electronic responses meet in cuprate superconductors," Phys. Rev. B **75**, 224508.

Chowdhury, Debanjan, Yochai Werman, Erez Berg, and T. Senthil, 2018, "Translationally Invariant Non-Fermi-Liquid Metals with Critical Fermi Surfaces: Solvable Models," Phys. Rev. X **8**, 031024.

Chu, J.-H., J. G. Analytis, C. Kucharczyk, and Ian R. Fisher, 2009, "Determination of the phase diagram of the electron-doped superconductor $Ba(Fe_{1-x}Co_x)_2As_2$," Phys. Rev. B **79**, 014506.

Damascelli, A., Z. Hussain, and Z.-X. Shen, 2003, "Angle-resolved photoemission studies of the cuprate superconductors," Rev. Mod. Phys. **75**, 473.

Emery, V. J., 1987, "Theory of High-T_c Superconductivity in Oxides," Phys. Rev. Lett. **58**, 2794–2797.

Fauqué, B., Y. Sidis, V. Hinkov, S. Pailhès, C. T. Lin, X. Chaud, and P. Bourges, 2006, "Magnetic Order in the Pseudogap Phase of High-T_C Superconductors," Phys. Rev. Lett. **96**, 197001.

Graf, J., *et al.*, 2007, "Universal High Energy Anomaly in the Angle-Resolved Photoemission Spectra of High Temperature Superconductors: Possible Evidence of Spinon and Holon Branches," Phys. Rev. Lett. **98**, 067004.

Hertz, J. A., 1976, "Quantum critical phenomena," Phys. Rev. B **14**, 1165.

Hohenberg, P. C., and B. I. Halperin, 1977, "Theory of dynamical critical phenomena," Rev. Mod. Phys. **49**, 435.

Hou, Changtao, and Chandra M. Varma, 2016, "Phase diagram and correlation functions of the two-dimensional dissipative quantum *XY* model," Phys. Rev. B **94**, 201101.

Hussey, N. E., R. A. Cooper, Xu Xiaofong, Y. Wang, I. Mouzopoulu, B. Vignolle, and C. Proust, 2011, "Dichotomy in the *T*-linear resistivity in hole-doped cuprates," Phil. Trans. R. Soc. A **369**, 1626.

Kadowaki, K., and S. B. Woods, 1986, "Universal relationship of the resistivity and specific heat in heavy-fermion compounds," Solid State Commun. **58**, 507–509.

Kaminski, A., *et al.*, 2002, "Spontaneous breaking of time-reversal symmetry in the pseudogap state of a high-T_c superconductor," Nature (London) **416**, 610–613.

Kaminski, A., *et al.*, 2005, "Momentum anisotropy of the scattering rate in cuprate superconductors," Phys. Rev. B **71**, 014517.

Kosterlitz, J. M., 1974, "The critical properties of the two-dimensional *xy* model," J. Phys. C **7**, 1046.

Lee, Patrick A., Naoto Nagaosa, and Xiao-Gang Wen, 2006, "Doping a Mott insulator: Physics of high-temperature superconductivity," Rev. Mod. Phys. **78**, 17–85.

Legros, A., *et al.*, 2019, "Universal *T*-linear resistivity and Planckian dissipation in overdoped cuprates," Nat. Phys. **15**, 142.

Leridon, B., P. Monod, D. Colson, and A. Forget, 2009, "Thermodynamic signature of a phase transition in the pseudogap phase of $YBa_2Cu_3O_x$ high-T_C superconductor," Europhys. Lett. **87**, 17011.

Lu, Xiaobo, *et al.*, 2019, "Superconductors, orbital magnets, and correlated states in magic angle bilayer graphene," arXiv:1903.06513.

Lubashevsky, Y., LiDong Pan, T. Kirzhner, G. Koren, and N. P. Armitage, 2014, "Optical Birefringence and Dichroism of Cuprate Superconductors in the THz Regime," Phys. Rev. Lett. **112**, 147001.

Lv, B., M. Gooch, B. Lorenz, F. Chen, A. M. Guloy, and C. W. Chu, 2009, "The superconductor $K_xSr_{1-x}Fe_2As_2$: Normal state and superconducting properties," New J. Phys. **11**, 025013.

Mattheiss, L. F., 1987, "Electronic Band Properties and Superconductivity in $La_{2-y}x_yCuO_4$," Phys. Rev. Lett. **58**, 1028–1030.

Meevasana, W., F. Baumberger, K. Tanaka, F. Schmitt, W. R. Dunkel, D. H. Lu, S.-K. Mo, H. Eisaki, and Z.-X. Shen, 2008, "Extracting the spectral function of the cuprates by a full two-dimensional analysis: Angle-resolved photoemission spectra of $Bi_2Sr_2CaCu_2O_6$," Phys. Rev. B **77**, 104506.

Michon, B., *et al.*, 2019, "Thermodynamic signatures of quantum criticality in cuprate superconductors," Nature (London) **567**, 218.

Mitrano, M., *et al.*, 2018, "Anomalous density fluctuations in a strange metal," *Proc. Natl. Acad. Sci. U.S.A.* 115, 5392–5396.

Miyake, K., T. Matsuura, and C. M. Varma, 1989, "Relation between resistivity and effective mass in heavy-fermion and A15 compounds," Solid State Commun. **71**, 1149–1153.

Miyake, K., S. Schmitt-Rink, and C. M. Varma, 1986, "Spin-fluctuation-mediated even-parity pairing in heavy-fermion superconductors," Phys. Rev. B **34**, 6554–6556.

Moriya, T., 1985, *Spin Fluctuations in Itinerant Electron Magnetism* (Springer-Verlag, Berlin).

Mukherjee, A., *et al.*, 2019, "Linear dichroism infrared resonance in over-, under-, and optimally-doped cuprate superconductors," arXiv:1907.08649.

Murayama, H., Y. Sato, R. Kurihara, S. Kasahara, Y. Mizukami, Y. Kasahara, H. Uchiyama, A. Yamamoto, E. G. Moon, and J. Cai, 2018, "Diagonal nematicity in the pseudogap phase of $HgBa_2CuO_{4+\delta}$," arXiv:1805.00276.

Noziéres, P., 1960, *Theory of Interacting Fermi Systems* (Benjamin, New York).

Polshyn, H., M. Yankowitz, S. Chen, Y. Zhang, K. Watanabe, T. Taniguchi, C. R. Dean, and A. F. Young, 2019, "Spin dynamics near a putative antiferromagnetic quantum critical point in Cu substituted $BaFe_2As_2$ and its relation to high-temperature superconductivity," arXiv:1902.00763.

Prange, Richard E., and Leo P. Kadanoff, 1964, "Transport theory or electron-phonon interactions in metals," Phys. Rev. **134**, A566–A580.

Sachdev, Subir, and Jinwu Ye, 1993, "Gapless Spin-Fluid Ground State in a Random Quantum Heisenberg Magnet," Phys. Rev. Lett. **70**, 3339–3342.

Sato, Y., *et al.*, 2017, "Thermodynamic evidence for a nematic phase transition at the onset of the pseudogap in $YBa_2Cu_3O_y$," Nat. Phys. **13**, 1074–1078.

Scalapino, D. J., 2012, "A common thread: The pairing interaction for unconventional superconductors," Rev. Mod. Phys. **84**, 1383–1417.

Schröder, A., G. Aeppli, E. Bucher, R. Ramazashvili, and P. Coleman, 1998, Phys. Rev. Lett. **80**, 5623.

Sebastian, S., and C. Proust, 2015, "Quantum oscillations in hole-doped cuprates," Annu. Rev. Condens. Matter Phys. **6**, 411.

Shekhter, A., and C. M. Varma, 2009, "Long-wavelength correlations and transport in a marginal Fermi liquid," Phys. Rev. B **79**, 045117.

Shekhter, Arkady, B. J. Ramshaw, Ruixing Liang, W. N. Hardy, D. A. Bonn, Fedor F. Balakirev, Ross D. McDonald, Jon B. Betts, Scott C. Riggs, and Albert Migliori, 2013, "Bounding the pseudogap with a line of phase transitions in $YBa_2Cu_3O_{6+\delta}$," Nature (London) **498**, 75–77.

Shibauchi, T., A. Carrington, and Y. Matsuda, 2014, "A quantum critical point lying beneath the superconducting dome in iron pnictides," Annu. Rev. Condens. Matter Phys. **5**, 113–135.

Si, Q., S. Rabello, K. Ingersent, and J. Lleweilun Smith, 2001, Nature (London) **413**, 804.

Valla, T., A. V. Fedorov, P. D. Johnson, Q. Li, G. D. Gu, and N. Koshizuka, 2000, "Temperature Dependent Scattering Rates at the Fermi Surface of Optimally Doped $Bi_2Sr_2CaCu_2O_{8+}$," Phys. Rev. Lett. **85**, 828.

Varma, C. M., 1985, "Phenomenological Aspects of Heavy Fermions," Phys. Rev. Lett. **55**, 2723–2726.

Varma, C. M., 1997, "Non-Fermi-liquid states and pairing instability of a general model of copper oxide metals," Phys. Rev. B **55**, 14554–14580.

Varma, C. M., 2015, "Quantum Criticality in Quasi-Two-Dimensional Itinerant Antiferromagnets," Phys. Rev. Lett. **115**, 186405.

Varma, C. M., and Elihu Abrahams, 2001, "Effective Lorentz Force due to Small-Angle Impurity Scattering: Magnetotransport in High-T_c Superconductors," Phys. Rev. Lett. **86**, 4652–4655.

Varma, C. M., P. B. Littlewood, S. Schmitt-Rink, E. Abrahams, and A. E. Ruckenstein, 1989, "Phenomenology of the Normal State of Copper Oxide High-Temperature Superconductors," Phys. Rev. Lett. **63**, 1996–1999.

Varma, C. M., S. Schmitt-Rink, and E. Abrahams, 1987, "Charge transfer excitations and superconductivity in 'ionic' metals," Solid State Commun. **62**, 681.

Varma, C. M., and Lijun Zhu, 2015, "Specific heat and sound velocity at the relevant competing phase of high-temperature superconductors," Proc. Natl. Acad. Sci. U.S.A. **112**, 6331.

Varma, C. M., Lijun Zhu, and Almut Schröder, 2015, "Quantum critical response function in quasi-two-dimensional itinerant antiferromagnets," Phys. Rev. B **92**, 155150.

Varma, Chandra M., 2016, "Quantum-critical fluctuations in 2D metals: Strange metals and superconductivity in antiferromagnets and in cuprates," Rep. Prog. Phys. **79**, 082501.

Varma, Chandra M., 2017, "Dynamic structure function of some singular Fermi liquids," Phys. Rev. B **96**, 075122.

Varma, Chandra M., 2019, "Pseudogap and Fermi arcs in underdoped cuprates," Phys. Rev. B **99**, 224516.

von Löhneysen, H., 1996, "Non-Fermi-liquid behaviour in the heavy-fermion system ," J. Phys. Condens. Matter **8**, 9689.

von Löhneysen, H., A. Rosch, M. Vojta, and P. Wölfle, 2007, "Fermi-liquid instabilities at magnetic quantum phase transitions," Rev. Mod. Phys. **79**, 1015.

Xia, Jing, *et al.*, 2008, "Polar Kerr-Effect Measurements of the High-Temperature $YBa_2Cu_3O_{6+x}$ Superconductor: Evidence for Broken Symmetry near the Pseudogap Temperature," Phys. Rev. Lett. **100**, 127002.

Zaanen, J., Koenrad Schalm, Ya-Wen Sun, and Yan Liu, 2015, *Holographic Duality in Condensed Matter Physics* (Cambridge University Press, Cambridge, England).

Zhang, Jian, *et al.*, 2018, "Discovery of slow magnetic fluctuations and critical slowing down in the pseudogap phase of $YBa_2Cu_3O_y$," Sci. Adv. **4**, eaao5235.

Zhao, L., C. A. Belvin, R. Liang, D. A. Bonn, W. N. Hardy, N. P. Armitage, and D. Hsieh, 2017, "A global inversion-symmetry-broken phase inside the pseudogap region of $YBa_2Cu_3O_y$," Nat. Phys. **13**, 250.

Zhu, L., Vivek Aji, Arkady Shekhter, and C. M. Varma, 2008, "Universality of Single-Particle Spectra of Cuprate Superconductors," Phys. Rev. Lett. **100**, 057001.

Zhu, Lijun, Yan Chen, and Chandra M. Varma, 2015, "Local quantum criticality in the two-dimensional dissipative quantum *XY* model," Phys. Rev. B **91**, 205129.

Zhu, Lijun, Changtao Hou, and Chandra M. Varma, 2016, "Quantum criticality in the two-dimensional dissipative quantum *XY* model," Phys. Rev. B **94**, 235156.